Higgs boson mass effects in the process $\mu^+_{R(L)}\mu^-_{R(L)} \to W^+_L W^-_L$

J. K. Singhal* and Sardar Singh
Department of Physics, University of Rajasthan, Jaipur 302004, India

(Received 19 December 2000; revised manuscript received 9 March 2001; published 31 May 2001)

The process $\mu^+_{R(L)}\mu^-_{R(L)} \to W^+_L W^-_L$ is studied with a view to discern the Higgs boson mass effects. The helicity amplitudes are evaluated retaining muon mass terms and cancellation of possible bad high energy behavior is discussed. The results are examined in the context of the equivalence theorem. The Higgs boson mass effects in the differential cross section ($d\sigma/d\cos\theta$), total cross section (σ), and forward-backward asymmetry (A_{FB}) are presented for two cases: (i) $m_H < 2m_W$ and (ii) $m_H > 2m_W$. Near the W_L pair production threshold, both $d\sigma/d\cos\theta$ and σ increase with an increase in $\sqrt{s}$ for case (ii), while this trend is absent for case (i). Near resonance ($\sqrt{s} \approx m_H$), $d\sigma/d\cos\theta$ does not show an appreciable dependence on θ. For case (i) A_{FB} is always positive, while for case (ii) A_{FB} changes sign from negative to positive at $\sqrt{s} = m_H$. The A_{FB} decreases with an increase in m_H for any $\sqrt{s} > m_H$.

DOI: 10.1103/PhysRevD.64.013007 PACS number(s): 14.80.Bn, 12.15.−y

I. INTRODUCTION

The $SU(2)_L \times U(1)_Y$ standard model (SM) has successfully passed precision tests which at present are at a 0.1% level [1–3]. The masses of SM particles are generated by the Higgs mechanism [4], which results in at least one neutral scalar Higgs boson. The Higgs boson is also required for the cancellation of high-energy divergences [5].

In the SM the Higgs boson mass m_H is arbitrary; however there exist theoretical as well as indirect experimental bounds on m_H [6,7]. For the CERN e^+e^- collider LEP data collected in 1999, the recent 95% C.L. SM Higgs boson mass bound is $m_H > 107.7$ GeV [7,8].

Recently there has been much interest in the possibility of constructing a $\mu^+\mu^-$ collider and a survey of physics possibilities has been made [9–13]. The physics potential of a high-energy muon collider has opened the prospectus for a detailed study of a W-boson pair production in the process $\mu^+\mu^- \to W^+W^-$. For the process $l^+l^- \to W^+W^-$ (with $l = e$, μ, or τ), the Higgs boson contribution arises due to an s-channel Higgs boson exchange diagram (see Fig. 1). The process $e^+e^- \to W^+W^-$ has been studied in detail earlier [14–16]; however, the Higgs boson mass effects were not considered due to the smallness of m_e. The helicity consideration reveals that the Higgs boson contributes only for the $l^+_{R(L)}l^-_{R(L)}$ annihilation [where $R(L)$ refers to right(left) handed helicity states]. The helicity amplitudes for the process $\mu^+_{R(L)}\mu^-_{R(L)} \to W^+W^-$ in comparison to the process $e^+_{R(L)}e^-_{R(L)} \to W^+W^-$ are enhanced by a factor (m_μ/m_e), owing to the fact that the SM couplings of Higgs boson to fermions are proportional to the corresponding fermion mass. The Higgs boson plays an important role in the exact cancellation of bad high-energy behavior in the limit $\sqrt{s} \to \infty$ for the production of longitudinally polarized W's in the process $f\bar{f} \to W_L W_L$ (due to the s-wave amplitude) [5]. Recently the direct observation of longitudinally polarized W bosons has been reported and the measured fraction is 0.261 [17]. In view of these we consider the process $\mu^+_{R(L)}\mu^-_{R(L)} \to W^+_L W^-_L$ and analyze the effects of Higgs boson mass in (i) a differential cross section (angular distribution), (ii) a total cross section, and (iii) forward-backward asymmetry. The plan of the paper is as follows: In Sec. II, for the sake of completeness and defining our notations, we evaluate the helicity amplitudes retaining muon mass terms and discuss the cancellation of possible bad high energy behavior. The results are examined in the context of the equivalence theorem. The expressions for the cross sections and forward-backward asymmetry are obtained. In Sec. III, we analyze the Higgs boson mass effects and in Sec. IV we summarize our results.

II. HELICITY AMPLITUDES AND CROSS SECTIONS

A. The helicity amplitudes

The helicity amplitude for the process

$$\mu^-(k,\sigma) + \mu^+(\bar{k},\bar{\sigma}) \to W^-(q,\lambda) + W^+(\bar{q},\bar{\lambda}) \qquad (1)$$

(where the arguments indicate the four momenta and helicities of the respective particles) are calculated following the technique described by Hagiwara *et al.* [14] and using Ref. [18] in which relevant details for helicity amplitude calculations are described. We use standard model couplings, uni-

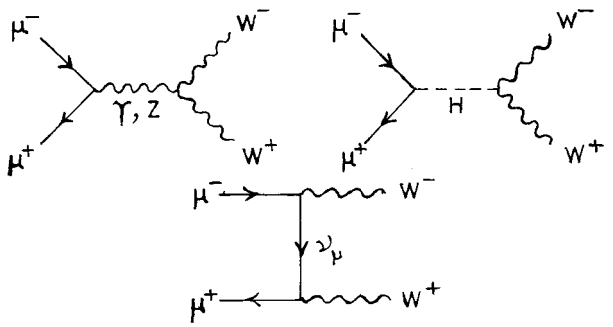

FIG. 1. s-channel γ, Z, and H-exchange diagram and t-channel, ν-exchange diagram.

*On leave from Govt. College, Sawai Madhopur, Rajasthan. Email address: jksinghal@hotmail.com

TABLE I. The explicit form of the $A^{\gamma,Z}_{\lambda\bar{\lambda}}$, $A'^{\gamma,Z}_{\lambda\bar{\lambda}}$, $B_{\lambda\bar{\lambda}}$, $B'_{\lambda\bar{\lambda}}$, $C_{\lambda\bar{\lambda}}$, $C'_{\lambda\bar{\lambda}}$, and $H_{\lambda\bar{\lambda}}$ coefficients.

$(\lambda,\bar{\lambda})$	$A^{\gamma,Z}_{\lambda\bar{\lambda}}$	$B_{\lambda\bar{\lambda}}$	$C_{\lambda\bar{\lambda}}$	$A'^{\gamma,Z}_{\lambda\bar{\lambda}}$	$B'_{\lambda\bar{\lambda}}$	$C'_{\lambda\bar{\lambda}}$	$H_{\lambda\bar{\lambda}}$
(+,0)	2γ	2γ	$2(1+\beta)/\gamma$	1	1	$1-(\beta+\sigma)\beta^2$	–
(0,−)						$1-(\beta-\sigma)\beta^2$	
(0,+)	2γ	2γ	$2(1-\beta)/\gamma$	1	1	$1+(\beta+\sigma)\beta^2$	–
(−,0)						$1+(\beta-\sigma)\beta^2$	
(+,+)	1	1	$1/\gamma^2$	$1/2\gamma$	$\cos\theta/2\gamma$	$\cos\theta/2\gamma^3$	$-1/4\gamma$
(−,−)							
(0,0)	$2\gamma^2+1$	$2\gamma^2$	$2/\gamma^2$	$(2\gamma^2+1)/2\gamma$	$\gamma(\beta+\cos\theta)$	$\cos\theta/\gamma^3$	$\gamma(1+\beta^2)/4$

tary gauge propagators, and Jacob-Wick phase conventions. The contributions to the helicity amplitude from various graphs in Fig. 1 are separated as [19]

$$M_{\sigma\bar{\sigma},\lambda\bar{\lambda}}(\theta)=\sqrt{2}e^2\tilde{M}_{\sigma\bar{\sigma},\lambda\bar{\lambda}}(\theta)d^{J_0}_{\Delta\sigma,\Delta\lambda}(\theta) \tag{2}$$

where $\Delta\lambda=\lambda-\bar{\lambda}$, $\Delta\sigma=(\sigma-\bar{\sigma})/2$, $J_0=\max(|\Delta\sigma|,|\Delta\lambda|)$ is the minimum angular momentum of the system, and θ is the scattering angle of W^- with respect to the μ^- direction in the $\mu^+\mu^-$ c.m. frame. The $d^{J_0}_{\Delta\sigma,\Delta\lambda}$ are the d functions [20]. The amplitude $\tilde{M}_{\sigma\bar{\sigma},\lambda\bar{\lambda}}$ includes contributions from γ, Z, H, and ν exchange diagrams of Fig. 1, i.e.,

$$\tilde{M}=\tilde{M}^{\gamma}+\tilde{M}^{Z}+\tilde{M}^{H}+\tilde{M}^{\nu}. \tag{3}$$

The explicit form of these contributions [with $\beta=\sqrt{1-(4m_W^2/s)}$, $\gamma=\sqrt{s}/2m_W$, $\sqrt{s}=$total c.m. energy, m_μ, m_W, m_Z, and m_H the masses of muon, W, Z, and H bosons, respectively, and Γ_H the decay width of the H boson [21]], are found to be

$$\tilde{M}^{\gamma}=-\beta\delta_{|\Delta\sigma|,1}A^{\gamma}_{\lambda\bar{\lambda}}\delta_{J_0,1}-\beta\delta_{\Delta\sigma,0}\frac{\sqrt{2}m_\mu}{m_W}A'^{\gamma}_{\lambda\bar{\lambda}}(\delta_{J_0,1}+\cos\theta\,\delta_{J_0,0}), \tag{4}$$

$$\tilde{M}^{Z}=\beta\left(\delta_{|\Delta\sigma|,1}-\frac{\delta_{\Delta\sigma,-1}}{2\sin^2\theta_W}\right)A^{Z}_{\lambda\bar{\lambda}}\frac{s}{s-m_Z^2}\delta_{J_0,1}+\beta\delta_{\Delta\sigma,0}\frac{\sqrt{2}m_\mu}{m_W}\left(1-\frac{1}{4\sin^2\theta_W}\right)A'^{Z}_{\lambda\bar{\lambda}}\frac{s}{s-m_Z^2}\times(\delta_{J_0,1}+\cos\theta\,\delta_{J_0,0}), \tag{5}$$

$$\tilde{M}^{H}=-\delta_{\Delta\sigma,0}\frac{\sqrt{2}m_\mu}{m_W}\frac{1}{2\sin^2\theta_W}H_{\lambda\bar{\lambda}}\frac{s}{s-m_H^2+i\Gamma_H m_H}\delta_{J_0,0}, \tag{6}$$

and

$$\tilde{M}^{\nu}=\frac{-\sqrt{2}}{\sin^2\theta_W}\frac{\delta_{J_0,2}}{1+\beta^2-2\beta\cos\theta}\left(\delta_{\Delta\sigma,-1}+\delta_{\Delta\sigma,0}\frac{\sqrt{2}m_\mu}{m_W}\frac{1}{2\sqrt{3}\gamma}\right)+\frac{1}{2\sin^2\theta_W\beta}\left[\begin{array}{c}\delta_{\Delta\sigma,-1}\left(B_{\lambda\bar{\lambda}}-\dfrac{C_{\lambda\bar{\lambda}}}{1+\beta^2-2\beta\cos\theta}\right)\delta_{J_0,1}\\ +\delta_{\Delta\sigma,0}\dfrac{\sqrt{2}m_\mu}{m_W}\dfrac{1}{2}\left(B'_{\lambda\bar{\lambda}}-\dfrac{C'_{\lambda\bar{\lambda}}}{1+\beta^2-2\beta\cos\theta}\right)(\delta_{J_0,1}+\delta_{J_0,0})\end{array}\right] \tag{7}$$

where the coefficients $A^{\gamma,Z}_{\lambda\bar{\lambda}}$, $A'^{\gamma,Z}_{\lambda\bar{\lambda}}$, $B_{\lambda\bar{\lambda}}$, $B'_{\lambda\bar{\lambda}}$, $C_{\lambda\bar{\lambda}}$, $C'_{\lambda\bar{\lambda}}$, and $H_{\lambda\bar{\lambda}}$ are given in Table I. Here the terms without m_μ are the same as those in Ref. [14] and terms with m_μ arise due to retention of the muon mass [22]. In Eq. (4) and Eq. (5) there are nonzero contributions for the case $\Delta\sigma=0$. In this regard we note that in the limit of massless muons ($m_\mu\to0$), as a consequence of helicity conservation only the spin 1 components (and only the transverse one) of the current contribute; the spin zero and the longitudinal components disappear, i.e., the conservation of chirality forbids terms with $\Delta\sigma=0$, $J_0=0$. Then the γ and Z exchange contributions have only $J_0=1$ partial waves. These are given by the first term in both Eq. (4) and Eq. (5). However, when muon mass is not neglected, the nonconservation of chirality gives rise to contributions of $O(m_\mu)$ for the case $\Delta\sigma=0$ and $J_0=0$. This leads to the possibility of the process $\mu^+_{R(L)}\mu^-_{R(L)}\to W^+_L W^-_L$ considered here [23]. For this process $\Delta\sigma=0$, $\lambda=\bar{\lambda}=0$, and as such $J_0=\max(|\Delta\sigma|,|\Delta\lambda|)=0$. Therefore, from Eq. (4) to Eq. (7) we get

$$\tilde{M}^{\gamma}_{\sigma\sigma,00} = -\frac{\sqrt{2}m_\mu}{m_W}\beta\frac{2\gamma^2+1}{2\gamma}\cos\theta, \tag{8}$$

$$\tilde{M}^{Z}_{\sigma\sigma,00} = \frac{\sqrt{2}m_\mu}{m_W}\left(1-\frac{1}{4\sin^2\theta_W}\right)\frac{s}{s-m_Z^2}\beta\left(\frac{2\gamma^2+1}{2\gamma}\right)\cos\theta, \tag{9}$$

$$\tilde{M}^{H}_{\sigma\sigma,00} = -\frac{\sqrt{2}m_\mu}{m_W}\frac{1}{4\sin^2\theta_W}\frac{s}{s-m_H^2+i\Gamma_H m_H}\frac{\gamma(1+\beta^2)}{2}, \tag{10}$$

$$\tilde{M}^{\nu}_{\sigma\sigma,00} = \frac{\sqrt{2}m_\mu}{m_W}\frac{1}{4\sin^2\theta_W\beta} \times\left[\gamma(\beta+\cos\theta)-\frac{\cos\theta}{\gamma^3(1+\beta^2-2\beta\cos\theta)}\right]. \tag{11}$$

We examine the effects of the above terms in the cancellation of possible bad high energy behavior in the limit $\sqrt{s}\to\infty$ (i.e., $\beta\to1$ and $\gamma\to\infty$). Retaining only the divergent terms in Eq. (8) to Eq. (11), we find

$$\tilde{M}^{\gamma}_{\sigma\sigma,00} = -\frac{\sqrt{2}m_\mu}{m_W}\gamma\cos\theta, \tag{12}$$

$$\tilde{M}^{Z}_{\sigma\sigma,00} = \frac{\sqrt{2}m_\mu}{m_W}\left(1-\frac{1}{4\sin^2\theta_W}\right)\gamma\cos\theta, \tag{13}$$

$$\tilde{M}^{H}_{\sigma\sigma,00} = -\frac{\sqrt{2}m_\mu}{m_W}\frac{1}{4\sin^2\theta_W}\gamma, \tag{14}$$

$$\tilde{M}^{\nu}_{\sigma\sigma,00} = \frac{\sqrt{2}m_\mu}{m_W}\frac{1}{4\sin^2\theta_W}\gamma(1+\cos\theta). \tag{15}$$

Unlike the case when the muon mass is not considered [24], now we have a divergent $(\tilde{M}^{\gamma}+\tilde{M}^{Z}+\tilde{M}^{\nu})$ contribution, namely

$$\tilde{M}^{\gamma}_{\sigma\sigma,00}+\tilde{M}^{Z}_{\sigma\sigma,00}+\tilde{M}^{\nu}_{\sigma\sigma,00} = \frac{\sqrt{2}m_\mu}{m_W}\frac{1}{4\sin^2\theta_W}\gamma. \tag{16}$$

This is precisely canceled by the contribution $\tilde{M}^{H}_{\sigma\sigma,00}$ from Higgs boson exchange [Eq. (14)].

Furthermore, the individual terms in Eq. (8) to Eq. (11) appear to diverge in the limit $m_W\to0$. However, when the combined contribution $\tilde{M}^{\gamma}+\tilde{M}^{Z}+\tilde{M}^{H}+\tilde{M}^{\nu}$ is considered, then for $\sqrt{s}\gg m_W, m_Z, m_H$ [with $\gamma=\sqrt{s}/(2m_W)\gg1$, and $\beta\to1$], we get

$$\begin{aligned}\tilde{M}^{\gamma}_{\sigma\sigma,00}+\tilde{M}^{Z}_{\sigma\sigma,00}+\tilde{M}^{H}_{\sigma\sigma,00}+\tilde{M}^{\nu}_{\sigma\sigma,00} &= -\frac{\sqrt{2}m_\mu}{m_W}\frac{1}{4\sin^2\theta_W}\frac{\cos\theta}{(\sqrt{s}/2m_W)^3(2-2\cos\theta)} \\ &\propto m_\mu\frac{m_W^2}{(\sqrt{s})^3}.\end{aligned} \tag{17}$$

Thus the apparent divergence of the amplitudes in the limit $m_W\to0$ disappears when the total amplitude $(\tilde{M}^{\gamma}+\tilde{M}^{Z}+\tilde{M}^{H}+\tilde{M}^{\nu})$ is considered.

It would be of interest to understand the results of our calculations in the context of the equivalence theorem [25–27] which states that at an energy $(\sqrt{s})$ much larger than the vector boson mass (m_W), the W_L behaves much like the corresponding Higgs ghost ϕ [27]. In our case if $M(\mu^+_{R(L)}\mu^-_{R(L)}\to W_L^+W_L^-)$ is the amplitude for the process involving W_L and physical Higgs particles in the standard model, and if $M(\mu^+_{R(L)}\mu^-_{R(L)}\to\phi^+\phi^-)$ is the analogous amplitude for the scalar field theory, then for m_H, $\sqrt{s}\gg m_W, m_Z$ we must have [27]

$$M(\mu^+_{R(L)}\mu^-_{R(L)}\to W_L^+W_L^-) = -M(\mu^+_{R(L)}\mu^-_{R(L)}\to\phi^+\phi^-) + O(m_W/\sqrt{s}). \tag{18}$$

In the limit $\sqrt{s}\gg m_W, m_Z$, using Eq. (8) to Eq. (11) in Eq. (2), expanding $\beta=\sqrt{1-(4m_W^2/s)}$ and using the fact that $d^0_{0,0}=1$, we get for $m_H>\sqrt{s}$, the amplitude in the standard model as

$$\begin{aligned}M(\mu^+_{R(L)}\mu^-_{R(L)}\to W_L^+W_L^-) &= \frac{e^2}{\sin^2\theta_W}\frac{m_\mu}{2m_W}\left[\frac{\sqrt{s}}{2m_W}\left(1+\frac{s}{m_H^2-s}\right)\right. \\ &\quad\left.+\frac{2m_W}{\sqrt{s}}\left(\cos\theta-\frac{s}{2(m_H^2-s)}\right)\right]\end{aligned} \tag{19}$$

where $O(m_W^2/s)$ and higher terms are ignored. We note that the first term in the square brackets gives an amplitude increasing with increases in $\sqrt{s}$ for $m_H>\sqrt{s}$ [28]. When we examine, in Sec. III, the cross section (σ) for this process near the $W^\pm$ production threshold for $m_H>\sqrt{s}$, the increasing trend of σ leads to a possibility of distinguishing between the $m_H<2m_W$ and $m_H>2m_W$ cases. Here, in order to check the results we evaluate $M(\mu^+_{R(L)}\mu^-_{R(L)}\to\phi^+\phi^-)$.

The process $f\bar{f}\to W_L^+W_L^-$, in the context of the equivalence theorem, has been discussed in detail by Veltman [27]. The Feynman diagrams contributing to the process $\mu^+_{R(L)}\mu^-_{R(L)}\to\phi^+\phi^-$ are shown in Fig. 2 (the neutrino mass is assumed to be nearly zero so that there is no contribution from neutrino exchange). Following Ref. [27] and using the calculational techniques described in Ref. [18] retaining the muon mass terms, we find in our notations the amplitude as

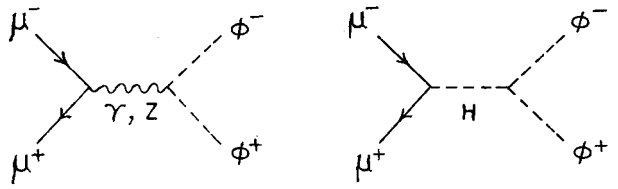

FIG. 2. The tree level diagrams contributing to the process $\mu^+\mu^-\to\phi^+\phi^-$.

$$M(\mu^+_{R(L)}\mu^-_{R(L)}\to\phi^+\phi^-) = -\frac{e^2}{\sin^2\theta_W}\frac{m_\mu}{2m_W}\left[\frac{\sqrt{s}}{2m_W}\frac{m_H^2}{m_H^2-s}+\frac{2m_W}{\sqrt{s}}\cos\theta \times\left(\frac{1+2\sin^2\theta_W}{2\cos^2\theta_W}\right)\right] \quad (20)$$

where $O(m_W^2/s)$ and higher terms are ignored. The first term in the square brackets of Eq. (20) is the same as the first term in the square brackets of Eq. (19), thereby confirming the requirements of the equivalence theorem [Eq. (18)].

B. The cross sections

For analyzing the Higgs boson mass effects in the process $\mu^+_{R(L)}\mu^-_{R(L)}\to W_L^+W_L^-$ we evaluate the following.

(i) The differential cross section [29]

$$\frac{d\sigma(\theta)}{d\cos\theta}=\frac{\beta}{128\pi s}|M_{\sigma\sigma,00}|^2. \quad (21)$$

(ii) The total cross section

$$\sigma=\int\frac{d\sigma(\theta)}{d\cos\theta}d(\cos\theta). \quad (22)$$

(iii) The forward-backward asymmetry

$$A_{FB}=\frac{\int_0^{\pi/2}\frac{d\sigma}{d\cos\theta}d(\cos\theta)-\int_{\pi/2}^{\pi}\frac{d\sigma}{d\cos\theta}d(\cos\theta)}{\int_0^{\pi/2}\frac{d\sigma}{d\cos\theta}d(\cos\theta)+\int_{\pi/2}^{\pi}\frac{d\sigma}{d\cos\theta}d(\cos\theta)}. \quad (23)$$

The detailed expressions for the $d\sigma/d\cos\theta$, σ, and A_{FB} are given in the Appendix.

III. HIGGS BOSON MASS EFFECTS

In order to study the Higgs boson mass effects in $d\sigma/d\cos\theta$, σ, and A_{FB}, we consider two cases: (i) $m_H<2m_W$ and (ii) $m_H>2m_W$ by taking representative values of m_H (between 115 GeV to 250 GeV). For numerical evaluation we take [30] $m_\mu=0.10566\,\text{GeV}$, $m_W=80.419$ GeV, $m_Z=91.118$ GeV, and $\sin^2\theta_W=0.23117$. The Higgs boson decay widths Γ_H are taken from Ref. [31], Γ_H $\sim$0.003, 0.02, 1.5, and 4 GeV for $m_H=115$, 150, 200, and 250 GeV, respectively.

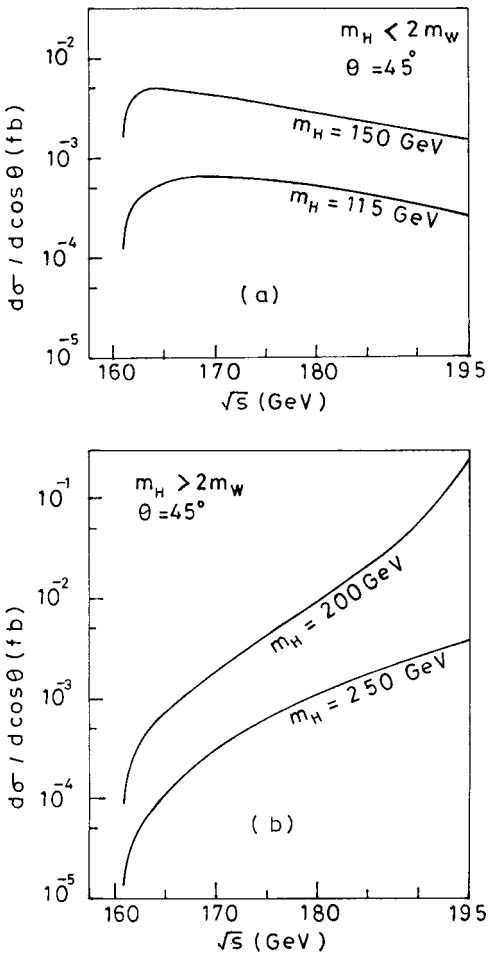

FIG. 3. The behavior of differential scattering cross section near W_L pair production threshold for (a) $m_H=115$ GeV, 150 GeV and (b) $m_H=200$ GeV, 250 GeV.

We first examine the behavior of differential cross section ($d\sigma/d\cos\theta$) and the total cross section (σ) near the W_L pair production threshold. The $d\sigma/d\cos\theta$ and σ as a function of $\sqrt{s}$ are plotted, respectively, in Fig. 3 and Fig. 4. We note that for case (ii) with $m_H>\sqrt{s}$ the $d\sigma/d\cos\theta$ [Fig. 3(b)] and σ [Fig. 4(b)] increase with increases in $\sqrt{s}$, while this trend is absent for case (i) [Figs. 3(a) and 4(a)]. We understand the shape of Figs. 3(b) and 4(b) by referring to Eq. (19). For $m_H>\sqrt{s}$ the dominant first term in the square brackets gives

$$M(\mu^+_{R(L)}\mu^-_{R(L)}\to W_L^+W_L^-)\propto\left[\frac{\sqrt{s}}{2m_W}\left(1+\frac{s}{m_H^2-s}\right)\right],$$

which leads to increasing $d\sigma/d\cos\theta$ and σ with increasing $\sqrt{s}$. Therefore measurement of the differential and/or total cross section near the W_L production threshold could possibly distinguish between (i) $m_H<2m_W$ and (ii) $m_H>2m_W$ cases.

In Fig. 5, we plot $d\sigma/d\cos\theta$ as a function of $\sqrt{s}$, including the near resonance ($m_H\sim\sqrt{s}$) region. For any $\sqrt{s}$ $>m_H$, the $d\sigma/d\cos\theta$ increases with increase in m_H. The

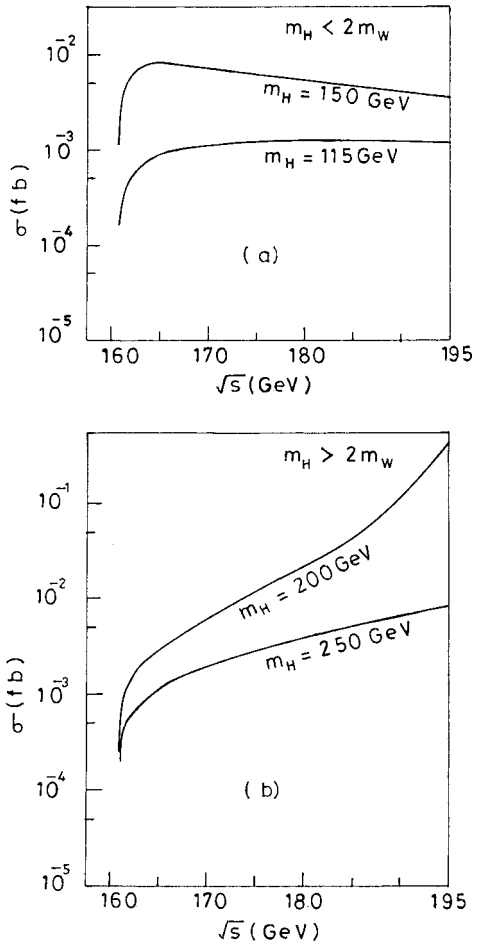

FIG. 4. The behavior of total cross section near W_L pair production threshold. (a) and (b) are the same as those in Fig. 3.

peaks occur at $\sqrt{s}=m_H$. Near resonance, the $d\sigma/d\cos\theta$ for $\sqrt{s}=200$ GeV and $m_H=195$ GeV to 205 GeV, is plotted in Fig. 6 for different θ values. We note that it does not show appreciable dependence on θ. The angular distribution ($d\sigma/d\cos\theta$ versus $\cos\theta$) at $\sqrt{s}=200$ GeV and $m_H=115$, 150, 200, and 250 GeV are shown in Fig. 7. We note that at resonance (i.e., $\sqrt{s}=m_H$) $d\sigma/d\cos\theta$ does not show variations with $\cos\theta$. For off resonance ($\sqrt{s}\neq m_H$), the $d\sigma/d\cos\theta$ dependence is as shown in Fig. 7.

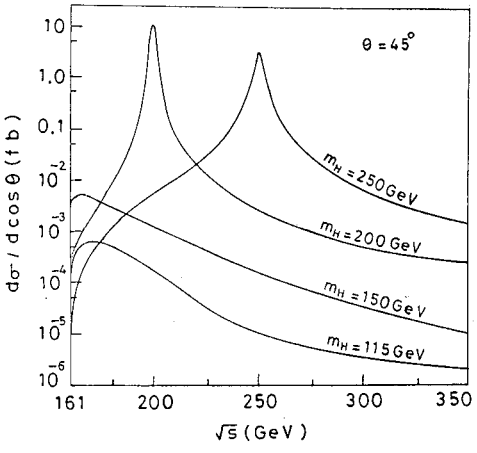

FIG. 5. The differential cross section ($d\sigma/d\cos\theta$) versus $\sqrt{s}$ for $m_H=115$, 150, 200, and 250 GeV.

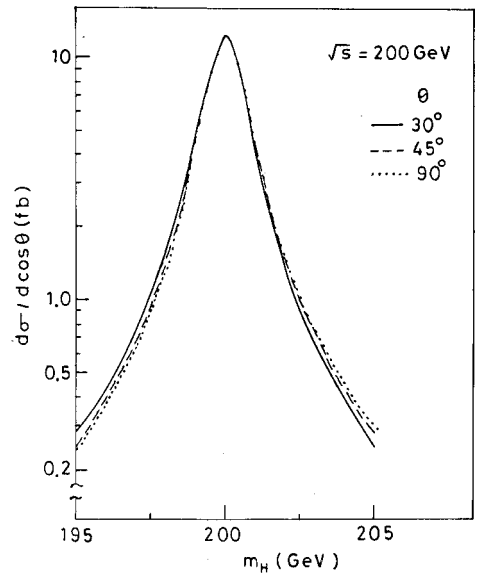

FIG. 6. The behavior of $d\sigma/d\cos\theta$ at $\sqrt{s}=200$ GeV, for $m_H=195$ to 205 GeV at different scattering angle θ.

For different values of m_H, the total cross section σ as a function of $\sqrt{s}$ is shown in Fig. 8. At any $\sqrt{s}>m_H$, the σ increases with increase in m_H for both (i) $m_H<2m_W$ and (ii) $m_H>2m_W$ cases.

The variation of forward-backward asymmetry (A_{FB}) with $\sqrt{s}$ is shown in Fig. 9. For the case $m_H<2m_W$, A_{FB} increases with an increase in $\sqrt{s}$ and is always positive. Further, the value of A_{FB} decreases with an increase in m_H. For the case $m_H>2m_W$, the A_{FB} decreases first with an increase

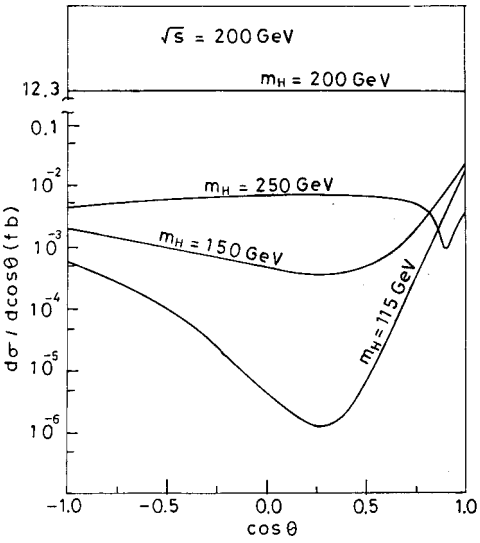

FIG. 7. The angular distribution ($d\sigma/d\cos\theta$ versus $\cos\theta$) at $\sqrt{s}=200$ GeV for $m_H=115$, 150, 200, and 250 GeV.

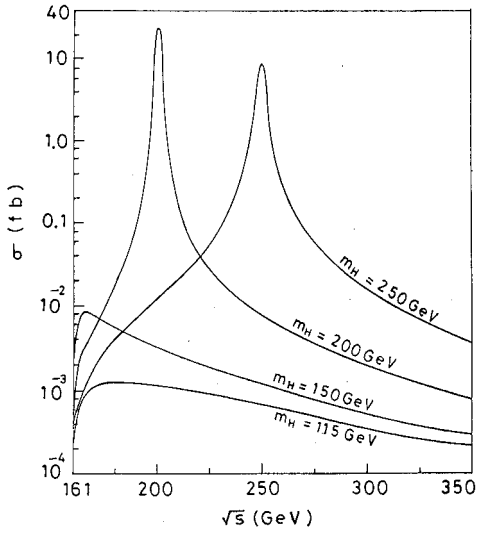

FIG. 8. The total cross section σ versus $\sqrt{s}$ for $m_H=115$, 150, 200, and 250 GeV.

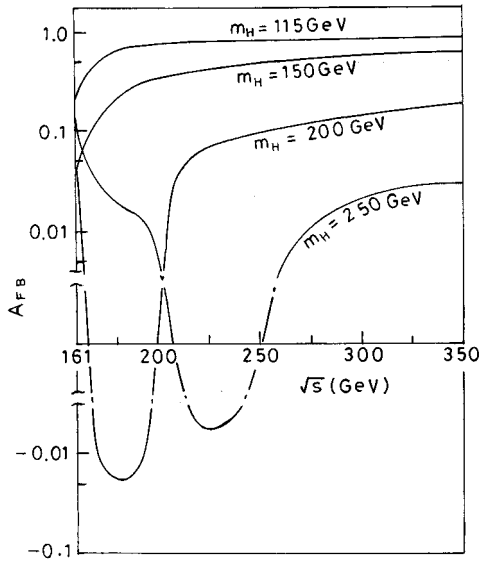

FIG. 9. The forward-backward asymmetry versus $\sqrt{s}$ for $m_H=115$, 150, 200, and 250 GeV.

in $\sqrt{s}$, becoming negative before $\sqrt{s}=m_H$ and again becoming positive just after $\sqrt{s}=m_H$. For $\sqrt{s}>m_H$, the A_{FB} remains positive. Furthermore, for any $\sqrt{s}>m_H$, the A_{FB} decreases with an increase in m_H.

IV. CONCLUSIONS

We considered the Higgs boson mass effects in the $d\sigma/d\cos\theta$, σ, and A_{FB} for the process $\mu^+_{R(L)}\mu^-_{R(L)} \rightarrow W_L^+ W_L^-$, with (i) $m_H<2m_W$ and (ii) $m_H>2m_W$. Near the W_L pair production threshold, both $d\sigma/\cos\theta$ and σ increases with an increase in $\sqrt{s}$ for case (ii), while this trend is absent for case (i). As such, measurements of $d\sigma/d\cos\theta$, σ near production threshold could possibly distinguish between the two cases.

The $d\sigma/d\cos\theta$ and σ for any $\sqrt{s}>m_H$ increases with an increase in m_H. For $\sqrt{s}\approx m_H$, the angular distribution ($d\sigma/d\cos\theta$ versus $\cos\theta$) does not exhibit appreciable dependence on θ. The forward-backward asymmetry A_{FB} for the $m_H<2m_W$ increases with an increase in $\sqrt{s}$ and always remains positive. For $m_H>2m_W$, A_{FB} first decreases, becoming negative with an increase in $\sqrt{s}$. For $\sqrt{s}\approx m_H$ the A_{FB} is negative just before $m_H=\sqrt{s}$ and is positive just after $m_H=\sqrt{s}$. The A_{FB} decreases with an increase in m_H for $\sqrt{s}>m_H$.

ACKNOWLEDGMENTS

J.K.S. acknowledges the financial assistance received from UGC, New Delhi and Director, College Education, Jaipur for granting academic leave. We thank Professor B. K. Sharma, Professor N. K. Sharma, and Dr. A. K. Nagawat for providing computer facilities.

APPENDIX

(i) The expression for the differential cross section ($d\sigma/d\cos\theta$) is

$$\frac{d\sigma(\theta)}{d\cos\theta}=\frac{\beta}{128\pi s}\frac{4e^4m_\mu^2}{m_W^2}[A_1(\theta)+B_1(\theta)+C_1(\theta)] \tag{A1}$$

where

$$A_1(\theta)=\left[\begin{array}{l}\beta\left\{\dfrac{2\gamma^2+1}{2\gamma}\left(m_Z^2-\dfrac{s}{4\sin^2\theta_W}\right)\dfrac{1}{s-m_Z^2}\right\}\cos\theta \\ +\dfrac{1}{4\sin^2\theta_W\beta}\left\{\gamma(\beta+\cos\theta)-\dfrac{\cos\theta}{\gamma^3(1+\beta^2-2\beta\cos\theta)}\right\}\end{array}\right]^2, \tag{A2}$$

$$B_1(\theta)=\frac{1}{(8\sin^2\theta_W)^2}\left[\frac{\{s\gamma(1+\beta^2)\}^2}{\{(s-m_H^2)^2+(\Gamma_H m_H)^2\}}\right], \tag{A3}$$

and

$$C_1(\theta)=-\left[\begin{array}{l}\beta\left\{\left(\frac{2\gamma^2+1}{2\gamma}\right)\left(m_Z^2-\frac{s}{4\sin^2\theta_W}\right)\frac{1}{s-m_Z^2}\right\}\cos\theta \\ +\frac{1}{4\sin^2\theta_W\beta}\left\{\gamma(\beta+\cos\theta)-\frac{\cos\theta}{\gamma^3(1+\beta^2-2\beta\cos\theta)}\right\}\end{array}\right]\frac{1}{4\sin^2\theta_W}\left[\frac{s\gamma(1+\beta^2)(s-m_H^2)}{(s-m_H^2)^2+(\Gamma_H m_H)^2}\right]. \tag{A4}$$

(ii) The expression for the total cross section σ is

$$\sigma=\frac{\beta}{128\pi s}\frac{8e^4m_\mu^2}{3m_W^2}[A_2+B_2+C_2], \tag{A5}$$

where

$$A_2=\left[\begin{array}{l}\left\{\beta\left(\frac{2\gamma^2+1}{2\gamma}\right)\left(m_Z^2-\frac{s}{4\sin^2\theta_W}\right)\frac{1}{s-m_Z^2}\right\}^2 \\ +\left(\frac{\gamma}{4\sin^2\theta_W\beta}\right)^2\left\{\frac{2}{\gamma^2}+\left(1+3\beta^2+\frac{1}{\gamma^4}\right)\left[1+\frac{3}{2\gamma^4\beta^2}\left(1+\frac{1+\beta^2}{2\beta}\log\frac{1-\beta}{1+\beta}\right)\right]\right\} \\ +\left(\frac{2\gamma^2+1}{4\sin^2\theta_W}\right)\left(m_Z^2-\frac{s}{4\sin^2\theta_W}\right)\frac{1}{s-m_Z^2}\left\{1+\frac{3(1+\beta^2)}{4\gamma^4\beta^2}\left(1+\frac{1+\beta^2}{2\beta}\log\frac{1-\beta}{1+\beta}\right)\right\}\end{array}\right], \tag{A6}$$

$$B_2=\frac{3}{(8\sin^2\theta_W)^2}\left[\frac{\{s\gamma(1+\beta^2)\}^2}{\{(s-m_H^2)^2+(\Gamma_H m_H)^2\}}\right], \tag{A7}$$

and

$$C_2=\frac{-3\gamma}{(4\sin^2\theta_W)^2}\left[\frac{s\gamma(1+\beta^2)(s-m_H^2)}{\{(s-m_H^2)^2+(\Gamma_H m_H)^2\}}\right]\left[1+\frac{1}{2\gamma^4\beta^2}\left\{1+\frac{1+\beta^2}{2\beta}\log\frac{1-\beta}{1+\beta}\right\}\right]. \tag{A8}$$

(iii) The expression for forward-backward asymmetry is found to be

$$A_{FB}=\left(\frac{3}{4\sin^2\theta_W}\right)\frac{N}{D}, \tag{A9}$$

where the numerator N is

$$N=\left\langle\begin{array}{l}\beta\left(\frac{2\gamma^2+1}{2}\right)\left(m_Z^2-\frac{s}{4\sin^2\theta_W}\right)\frac{1}{s-m_Z^2}\left\{1+\frac{1}{2\gamma^4\beta^2}\left[1+\frac{(1+\beta^2)^2}{2\beta^2}\log\frac{1-\beta^2}{1+\beta^2}\right]\right\} \\ +\left(\frac{\gamma^2}{4\sin^2\theta_W\beta}\right)\left\{1+\frac{1}{2\gamma^4\beta^2}\left(1+(1+\beta^2)\left[1+\left(1+3\beta^2+\frac{1}{\gamma^4}\right)\frac{1}{2\beta^2}\log\frac{1-\beta^2}{1+\beta^2}\right]\right)\right\} \\ -\left(\frac{s\gamma(1+\beta^2)(s-m_H^2)}{2\{(s-m_H^2)^2+(\Gamma_H m_H)^2\}}\right) \\ \times\left\{\beta\left(\frac{2\gamma^2+1}{2\gamma}\right)\left(m_Z^2-\frac{s}{4\sin^2\theta_W}\right)\frac{1}{s-m_Z^2}+\left(\frac{\gamma}{4\sin^2\theta_W\beta}\right)\left(1+\frac{1+\beta^2}{2\gamma^4\beta^2}\log\frac{1-\beta^2}{1+\beta^2}\right)\right\}\end{array}\right\rangle, \tag{A10}$$

and the denominator D is

$$D=\left[\begin{array}{l}\left\{\beta\left(\frac{2\gamma^2+1}{2\gamma}\right)\left(m_Z^2-\frac{s}{4\sin^2\theta_W}\right)\frac{1}{s-m_Z^2}\right\}^2 \\ +\left(\frac{\gamma}{4\sin^2\theta_W\beta}\right)^2\left\{\frac{2}{\gamma^4}+\left(1+3\beta^2+\frac{1}{\gamma^4}\right)\left[1+\frac{3}{2\gamma^4\beta^2}\left(1+\frac{1+\beta^2}{2\beta}\log\frac{1-\beta}{1+\beta}\right)\right]\right\} \\ +\left[\left(\frac{2\gamma^2+1}{4\sin^2\theta_W}\right)\left(m_Z^2-\frac{s}{4\sin^2\theta_W}\right)\frac{1}{s-m_Z^2}\right]\left[1+\frac{3(1+\beta^2)}{4\gamma^4\beta^2}\left(1+\frac{1+\beta^2}{2\beta}\log\frac{1-\beta}{1+\beta}\right)\right] \\ +\frac{3}{(8\sin^2\theta_W)^2}\frac{s\gamma^2(1+\beta^2)}{\{(s-m_H^2)^2+(\Gamma_H m_H)^2\}} \\ \times\left\{s(1+\beta^2)-4(s-m_H^2)\left[1+\frac{1}{2\gamma^4\beta^2}\left(1+\frac{1+\beta^2}{2\beta}\log\frac{1-\beta}{1+\beta}\right)\right]\right\}\end{array}\right]. \quad \text{(A11)}$$

[1] S. L. Glashow, Nucl. Phys. **22**, 579 (1961); S. Weinberg, Phys. Rev. Lett. **19**, 1264 (1967); A. Salam, in *Proceedings of the 8th Noble Symposium*, Stockholm, 1968, edited by N. Svartholm (Almqvist & Wiskell, Stockholm, 1968), p. 367.

[2] For a recent review see M. K. Gaillard, P. D. Grannis, and F. J. Sciulli, Rev. Mod. Phys. **71**, S96 (1999); M. Herrero, ''The Standard Model,'' hep-ph/9812242.

[3] J. Erler and P. Langacker, Eur. Phys. J. C **15**, 95 (2000); S. Bethke, ''Standard Model Physics at LEP,'' hep-ex/0001023; W. Marciano, ''Precision Electroweak Measurement and New Physics,'' hep-ph/9902332.

[4] P. W. Higgs, Phys. Lett. **12**, 132 (1964); Phys. Rev. Lett. **13**, 508 (1964); Phys. Rev. **145**, 1156 (1966).

[5] The quadratic divergences in $W_LW_L\to W_LW_L$ scattering and linear divergences in $f\bar{f}\to W_LW_L$ are precisely canceled by the Higgs boson contribution. See C. Quigg, Acta Phys. Pol. B **30**, 2145 (1999); M. Sipra and P. M. Zerwas, ''Electroweak Symmetry Breaking and Higgs Physics,'' hep-ph/9803257.

[6] C. Kolda and H. Murayama, J. High Energy Phys. **07**, 035 (2000).

[7] P. Igo-Kemenes, Eur. Phys. J. C **15**, 274 (2000), and references therein.

[8] M. Kado, ''Cornering Higgs Boson at LEP,'' hep-ex/0005022.

[9] B. Grzadkowski, J. F. Gunion, and J. Pliszka, Nucl. Phys. **B583**, 49 (2000).

[10] D. Neuffer, ''Mu+Mu Colliders,'' CERN Yellow Report No. cernep/99-12.

[11] V. Barger, M. S. Berger, J. F. Gunion, and T. Han, Phys. Rev. D **55**, 142 (1997).

[12] M. S. Berger, ''Muon Collider Physics at Very High Energies,'' hep-ph/0001018; V. Barger *et al.*, ''Physics Goals of $\mu^+\mu^-$ Collider'' (Report of Physics Goals Working Group), hep-ph/9803258.

[13] J. K. Singhal, Sardar Singh, Ashok K. Nagawat, and N. K. Sharma, Phys. Rev. D **63**, 017302 (2001).

[14] K. Hagiwara, R. D. Peccei, D. Zeppenfeld, and K. Hikasa, Nucl. Phys. **B282**, 253 (1987). The references for earlier important contributions are given therein.

[15] W. Beenakker, F. A. Berends, and A. P. Chapovsky, Nucl. Phys. **B548**, 3 (1999); W. Beenakker and A. Denner, Int. J. Mod. Phys. A **9**, 4837 (1994).

[16] Sardar Singh, A. K. Nagawat, and N. K. Sharma, Mod. Phys. Lett. A **5**, 1717 (1990); A. K. Nagawat, Sardar Singh, and N. K. Sharma, Phys. Rev. D **42**, 2984 (1990).

[17] L3 Collaboration, M. Acciari *et al.*, Phys. Lett. B **474**, 194 (2000).

[18] F. M. Renard, *Basics of Electron Positron Collisions* (Edition Frontiers, Gif-sur-Yvette, France, 1981).

[19] We omit a sign factor ε which is not required in the Jacob-Wick phase convention; see the footnote on p. 263 of Ref. [14].

[20] M. E. Rose, *Elementary Theory of Angular Momentum* (Wiley, New York, 1957).

[21] We do not consider Γ_Z as we present our calculation for $\sqrt{s}>m_Z$ and inclusion of Γ_Z does not change our results.

[22] In Ref. [14], Higgs boson exchange contribution is not included and also lepton mass terms are neglected. We retain Higgs boson contribution and do not neglect muon mass.

[23] It may be noted that the cross section for this helicity combination is only $(m_\mu/m_W)^2\sim 10^{-6}$ of the unpolarized cross section.

[24] When $m_\mu=0$ is taken in Eq. (4) to Eq. (7), then in the limit $\sqrt{s}\to\infty$ (i.e., $\beta\to 1$ and $\gamma\to\infty$), one gets $(\tilde{M}^\gamma+\tilde{M}^Z+\tilde{M}^\nu)\to 0$ as discussed in detail in Ref. [14]. As such, the role of the Higgs boson in the cancellation of possible bad high energy behavior is not visible for the $m_\mu=0$ choice.

[25] B. W. Lee, C. Quigg, and H. Thacker, Phys. Rev. D **16**, 1519 (1977); J. M. Cornwall, D. N. Levin, and G. Tiktopoulous, *ibid.* **10**, 1145 (1974); Y.-P. Yao and C.-P. Yuan, *ibid.* **38**, 2237 (1988); S. Dawson and S. Willensbrock, *ibid.* **40**, 2880 (1989); M. S. Chanowitz and M. K. Gaillard, Nucl. Phys. **B261**, 379 (1985).

[26] H. Veltman, Phys. Rev. D **41**, 2294 (1990); J. Bagger and C. Schmidt, *ibid.* **41**, 264 (1990).

[27] H. Veltman, Phys. Rev. D **43**, 2236 (1991).

[28] The increasing trend lasts until resonance at $\sqrt{s}=m_H$ is achieved. After that the amplitude decreases. One may use it to explore unitarity bounds on m_H in a manner similar to that discussed by B. W. Lee, C. Quigg, and H. Thacker, Phys. Rev. D **16**, 1519 (1977). However, our aim in this paper is not to explore the unitarity related questions. We restrict ourselves to the investigation of the possible Higgs boson mass effects for

$m_H \leqslant 250$ GeV. The current 95% C.L. limit on Higgs boson mass is $m_H \leqslant 235$ GeV [J. Erler and P. Langacker, Eur. Phys. J. C **15**, 95 (2000)].

[29] Physics at LEP, LEP Jamboree, Geneva, 1985, edited by J. Ellis and R. D. Peccei, CERN Yellow Report No. 86-02, 1986, Vol. 2.

[30] Particle Data Group, D. E. Groom *et al.*, Eur. Phys. J. C **15**, 1 (2000).

[31] V. Barger, M. S. Berger, J. F. Gunion, and T. Hann, Phys. Rep. **286**, 1 (1997).